Kent Academic Repository

The structure of molten nickel chloride

R J Newport†, R A Howe and N D Wood
Department of Physics, University of Leicester, Leicester, LE1 7RH, UK

Abstract. The structure of molten $NiCl_2$ has been investigated by the scattering of neutrons from isotopically enriched samples. The three partial structure factors relating to Ni–Ni, Cl–Cl and Ni–Cl correlations and the three corresponding radial distribution functions have been determined from the experimental data. The results are compared with those obtained from earlier studies of 2:1 molten salts and are discussed in the context of polarisation and ion size effects.

1. Introduction

Detailed and unique information about the short-range chemical order in liquids which contain more than one chemical species can be obtained from neutron diffraction studies of isotopically enriched samples. Investigations into the structure of divalent metal chloride melts using this technique were begun in 1978 by Edwards *et al* and have now reached a particularly interesting stage of development.

The purpose of this paper is to report on an experimental study of the structure of molten $NiCl_2$ in which isotopic substitution of Ni was carried out and to discuss the detailed features of the three partial distribution functions obtained by this method in the context of other 2:1 molten salt studies.

$NiCl_2$ was chosen for study for four reasons. Firstly, the small size of the Ni^{2+} ion should enable this system to provide a sensitive test of the ion-size effects that have been proposed as a prime factor in determining the nature of the short-range order and coordination number. Secondly, in the crystalline form, $NiCl_2$ belongs to a group of compounds which possess a layer-type structure of the $CdCl_2$ type in which the Ni ions occupy rhombohedrally centred sites in octahedrally structured layers of chloride ions (Wyckoff 1963). The degree of covalency inherent in such structures is a subject of current interest. Thirdly, the electronic structure of Ni^{2+} is d^8 and is therefore quite different from s–p cations of comparable size (for example Mg^{2+}).

Finally, from the neutron diffraction point of view, $NiCl_2$ is a particularly favourable candidate to study in that the coherent scattering length of Ni isotopes varies widely and, in the case of ^{62}Ni, assumes a negative value of appreciable amplitude. It is therefore possible to achieve a substantially more favourable conditioning for the $NiCl_2$ system than that attainable for the other 2:1 systems that have been studied to date. This

† Present address: Neutron Division, Rutherford Appleton Laboratory, Chilton, Didcot, Oxon, OX11 0QX, UK.

suggests that the statistical accuracy which can be achieved for this system is significantly greater than that attainable in the others.

2. Experimental

From a single neutron scattering measurement on a liquid containing two species a and b one can obtain the total structure factor $F(Q)$ defined by

$$F(Q) = c_a^2 b_a^2 (S_{aa} - 1) + c_b^2 b_b^2 (S_{bb} - 1) + 2c_a c_b b_a b_b (S_{ab} - 1) \tag{1}$$

where c_a, c_b are the atomic concentrations of the two species; b_a, b_b are the coherent neutron scattering lengths and S_{aa}, S_{bb} and S_{ab} are the partial structure factors. These structure factors are related to the pair distribution functions $g_{\alpha\beta}$ by

$$S_{\alpha\beta}(Q) = 1 + (4\pi N/VQ) \int [g_{\alpha\beta}(r) - 1] r \sin Qr \, dr \tag{2}$$

where $\alpha, \beta = a$ or b and N is the total number of atoms in the volume V.

To determine the three partial structure factors it was necessary to measure the neutron scattering intensity from three samples of $NiCl_2$ in which the isotopic abundance of Ni (and thus the value of the coherent scattering length, b_{Ni}) was different. Details of the samples used in this study are listed in table 1 together with the degree of isotopic enrichment and the corresponding value of the coherent scattering length. The process of extracting $S_{\alpha\beta}(Q)$ and $g_{\alpha\beta}(r)$ from the data closely followed that described by Edwards *et al* (1975).

Table 1. Sample details: Containment, fused silica tubes (sealed; 3 atm argon) 7 mm internal diameter, 1.08 mm wall. Temperature, 1022 °C.

Sample	Composition (atomic %)				Effective coherent scattering lengths	
	^{Nat}Ni ($b = 1.03$)	^{60}Ni ($b = 0.282$)	^{62}Ni ($b = -0.87$)	^{Nat}Cl ($b = 0.958$)	$\bar{b}Ni$ (10^{-12} cm)	$\bar{b}Cl$ (10^{-12} cm)
Natural $NiCl_2$	33.3	—	—	66.7	1.03	0.958
'62' $NiCl_2$	1.1	—	32.2	66.7	−0.805	0.958
'Zero' $NiCl_2$	0.5	24.3	8.5	66.7	0.00	0.958

The isotopically enriched and natural samples were prepared, in an identical manner, in aqueous solution and then subsequently dried by heating under vacuum; the temperature being raised slowly to 250 °C. The samples were held at high temperature for several days whilst maintaining pressures of around 10^{-5} mbar. Tests carried out to determine the corrosive nature of molten $NiCl_2$ eliminated the use of the more favourable containers such as V, Ti–Zr (or even Ta, W and Mo). Fused silica containers, however, were shown to be chemically inert to molten $NiCl_2$. Handling and transfer of the samples to the containers was undertaken in an evacuable glove box filled with dried argon gas. The samples were sealed in dry argon at a pressure of one atmosphere at room temperature. This ensured that at the melting point, the overpressure of gas was in

excess of three atmospheres and was sufficient to avoid any sublimation of the salt which would otherwise occur close to the melting point.

3. Results

The total structure factors, $F(Q)$ for the three samples of $NiCl_2$ are presented in figure 1. They are obtained from the measured diffraction patterns after correcting the data for background, container, absorption, incoherent and multiple scattering. The three factors have been normalised using the standard vanadium calibration technique.
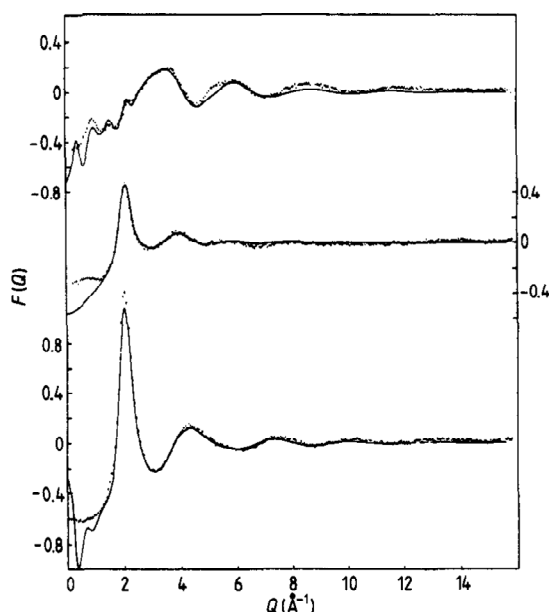

Figure 1. $F(Q)$ data for three samples of $NiCl_2$ at 1022 °C: natural Ni (upper curve), 'zero' Ni (middle curve) and ^{62}Ni (lower curve). The points are experimental and the curves are derived from the back transforms of the distribution functions shown in figure 3.

Figure 2 shows the three partial structure factors, $S_{\alpha\beta}(Q)$. These have been obtained by a direct solution of the three simultaneous equations which result from the application of equation 1. For the three samples

$$F(Q) \text{ 'Zero'} = 0.408[S_{ClCl}(Q) - 1]$$

$$F(Q) \text{ '62'} = 0.408\,[S_{ClCl}(Q) - 1] + 0.072[S_{NiNi}(Q) - 1] - 0.343[S_{NiCl}(Q) - 1]$$

$$F(Q) \text{ 'Nat'} = 0.408\,[S_{ClCl}(Q) - 1] + 0.118[S_{NiNi}(Q) - 1] + 0.439[S_{NiCl}(Q) - 1].$$

The $S_{ClCl}(Q)$ function is thus obtained directly from the 'Zero' Ni data while the other two follow from analysis of the ^{62}Ni and natural Ni data. It can be seen that the coefficient of the term involving $S_{NiNi}(Q)$ is invariably small and the experiment is consequently somewhat insensitive to the Ni–Ni partial. The poor separation that results from this is
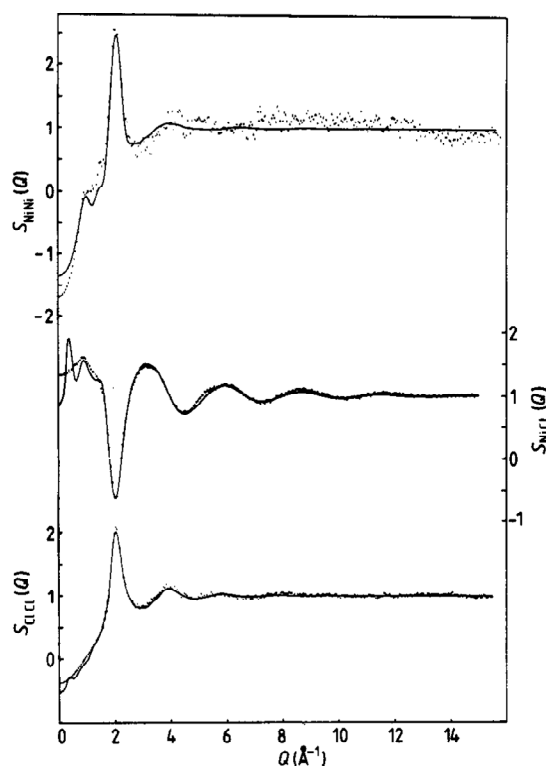
Figure 2. The partial structure factors for liquid $NiCl_2$.

readily observable in figure 2. Measurement of the neutron scattering from a $^{58}Ni^{37}Cl_2$ sample could be used to improve this resolution substantially but the preparation costs associated with such a double isotropic substitution sample are high. The alternative approach, of studying the iodide rather than the chloride, is currently being pursued, and this data will, amongst other things, provide more detailed information on the Ni–Ni partial in molten halides. The three partial structure factors have been Fourier transformed to produce the partial radial distribution functions shown in figure 3.

The effects of truncation and noise in the three $F(Q)$ functions and the uncertainty in the coherent scattering amplitudes and hence in the coefficients of equation (1) have been fully explored. The usual iterative procedure has been pursued to obtain the degree of self-consistency between the back-transforms and the original data that is shown in figure 1. Some points arising from this procedure are worth mentioning:

(i) The $g_{\alpha\beta}(r)$ were found to be relatively insensitive to the values of $S_{\alpha\beta}(0)$. In the absence of any published data on the isothermal compressibility of liquid $NiCl_2$, the three values for $S_{\alpha\beta}(0)$ were adopted in a self-consistent manner with reference to the compressibility of molten $ZnCl_2$. The uncertainty arising from the low-Q truncation is seen to be of no great consequence.

(ii) There is evidence to suggest that the pre-peak features shown in $S_{NiNi}(Q)$ are real. Any attempt to remove them produced a significant worsening of the agreement between the back transforms and the original data. Their presence results in a reduction in the height of and a narrowing of the principal peak in $g_{NiNi}(r)$.
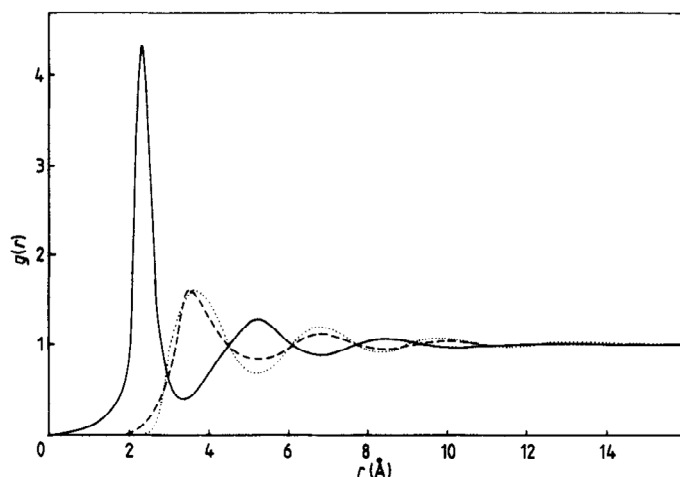
Figure 3. The radial distribution functions for liquid NiCl₂: full curve, g_{NiCl}; broken curve, g_{ClCl}; dotted curve, g_{NiNi}.

(iii) The details of $S_{NiNi}(Q)$ beyond a Q-value of around 6 Å^{-1} are unresolved but the $g_{NiNi}(r)$ proved to be insensitive to this region. The second peak at around 4 Å^{-1} is more significant in producing a distinct damping of $g_{NiNi}(r)$ at higher r-values and a slight shift to higher r of the principal peak in $g_{NiNi}(r)$.

(iv) The leading edge of the principal peak in $g_{NiCl}(r)$ does not fall rapidly to zero. A soft leading edge (as shown) or, alternatively a prepeak shoulder (not shown) were found necessary to obtain a good agreement in the mid-Q range of the back transform. The height of the principal peak was examined and for consistency, a value of 4.4 ± 0.3 was required.

A summary of the structural parameters for this system is given in table 2. The coordination numbers of β-type atoms about an α-type atom have been determined using the methods described by Waseda (1980).

Table 2. Structural parameters of liquid NiCl₂. Note (1) that the high value of $g_{\alpha\beta}(r)$ at the minimum precludes an accurate determination and (2) the data is very poorly matched to this symmetric function.

Structural parameters		Ni–Ni	Cl–Cl	Ni–Cl
Principal peak position in $g_{\alpha\beta}(r)$		3.66	3.48	2.32
(Å)	in $rg_{\alpha\beta}(r)$	3.88	3.62	2.34
	in $r^2g_{\alpha\beta}(r)$	4.00	3.80	2.36
Position of first minimum in $g_{\alpha\beta}(r)$				
(Å)		5.22	5.26	3.36
Coordination of β atoms around α in $g_{\alpha\beta}(r)$ by integration				
to first minimum in $g_{\alpha\beta}(r)$		6.7(1)	13.8(1)	4.9
over $rg(r)$ symmetric		5.1	6.7(2)	3.6(2)
over $r^2g(r)$ symmetric		6.0	9.0	3.8(2)
with high Q extrapolation		5.4	10.0	4.7
Most likely value		5.5 ± 0.5	9 ± 1	4.7 ± 0.2

4. Discussion

As described in the introduction, the crystalline form of $NiCl_2$ exhibits a sixfold, rhombo-hedral coordination of Cl ions around each Ni ion. Analysis of the melt data reveals that this coordination number is reduced in the liquid to a value of 4.7 ± 0.2. A comparison of the liquid data with the solid is presented in table 3. In the liquid phase, the ratio of $\bar{r}_{ClCl}/\bar{r}_{NiCl}$ is found to be 1.61 ± 0.02 in contrast to the value of 1.42 in the solid. Further-more, the liquid value corresponds, within experimental error, to that found in a true tetrahedral arrangement ($\sqrt{8/3} = 1.63$). The chlorine structure is little changed on

Table 3. Comparison of the structures of solid and liquid $NiCl_2$. $\bar{r}_{\alpha\beta}$ is the peak position in $r^2 g_{\alpha\beta}(r)$ and $\bar{n}_{\alpha\beta}$ is the cordination number of β atoms around an α atom.

	Ni–Ni	Cl–Cl	Ni–Cl
Solid			
$\bar{r}_{\alpha\beta}(\text{Å})$	3.54	3.54	2.50
$\bar{n}^{\alpha\beta}$	8	8	6
Liquid			
$\bar{r}_{\alpha\beta}(\text{Å})$	4.00 ± 0.05	3.80 ± 0.10	2.36 ± 0.02
$\bar{n}_{\alpha\beta}$	5.5 ± 0.5	9.0 ± 1.0	4.7 ± 0.2

melting with a small increase in the Cl–Cl separation and an unchanged coordination number. Finally, there is little or no penetration of like charge into the first coordination shell around the nickel. These facts when taken together suggest a model for the Ni structure that closely corresponds to that first proposed by Biggin and Enderby (1981) for Zn^{2+} in $ZnCl_2$. The Ni ions appear to occupy tetrahedrally coordinated sites within a closely packed Cl structure and the small size of the Ni ion precludes the possibility of like ion penetration.

The strong similarity between $g_{NiNi}(r)$ and $g_{ClCl}(r)$ and the close correspondence in the values of $\bar{r}_{\alpha\beta}$ (4.00 and 3.80 Å) is an important feature of this and other 2:1 systems. The antiphase relation between these and the $g_{NiCl}(r)$ are taken to be indicative of the charge cancellation of the system and evidence of an ionisation of the form $NiCl_2 \rightleftharpoons Ni^{2+} + 2Cl^-$. A simple Coulombic model would then suggest that the doubly charged Ni ions should reside at considerably greater separations than the singly charged Cl ions—a direct consequence of the extra repulsion associated with the double charge. That this does not occur is a clear indication of the need to go beyond a simple rigid ion model in these systems. Departures from simple Coulombic behaviour are also indicated by the structural features in the leading edge of the principal peak in $g_{NiCl}(r)$ described in the previous section.

In table 4, we compare the structural properties of $NiCl_2$ with those of other 2:1 chlorides. There are a number of important trends that become apparent from this comparison. Up to this point we have emphasised the similarity between liquid $NiCl_2$ and $ZnCl_2$. A clear distinction becomes apparent when one studies the heights of the principal peaks. In $NiCl_2$, the $--$ and $++$ peaks are about half the height of their counterparts in $ZnCl_2$. Table 4 reveals that this reduced peak height in the $++$ and $--$ partials is more correlated with temperature than with any ion size effects, and an

Table 4. Comparison of radial distribution functions of molten 2:1 chlorides. posn. denotes r-value of principal peak in $g_{\alpha\beta}(r)$, except in the cases of MgCl$_2$, NiCl$_2$ and MnCl$_2$ where posn. denotes r-values of the first peak in $r^2 g_{\alpha\beta}(r)$, $\bar{r}_{\alpha\beta}$. height denotes the value of $g_{\alpha\beta}(r)$ at the maximum and coord. number denotes the coordination of β atoms around an α atom obtained from $g_{\alpha\beta}(r)$ by one of several integral methods.

Chemical formula	Temp. (°C)	Cation radius (Å)	Cation–Cation			Anion–Anion			Cation–Anion		
			posn. (Å)	(height)	coord. number	posn. (Å)	(height)	coord. number	posn. (Å)	(height)	coord. number
MgCl$_2$[d]	725	0.66	3.81	(2.5)	5	3.56	(2.3)	12	2.42	(4.4)	4.3
NiCl$_2$	1022	0.69	4.00	(1.65)	5.5	3.80	(1.6)	9.0	2.36	(4.4)	4.7
ZnCl$_2$[b]	327	0.74	3.8	(2.8)	4.7	3.71	(3.1)	8.6	2.29	(5.2)	4.3
MnCl$_2$[d]	700	0.80		—		3.58		8.4	2.50		4.0
CaCl$_2$[b]	820	0.99	3.6	(2.5)	4.2	3.73	(2.1)	7.8	2.78	(4.2)	5.4
SrCl$_2$[c]	925	1.12	4.95	(1.62)	13.6	3.80	(1.88)	9.3	2.90	(2.9)	6.9
BaCl$_2$[a]	1025	1.35	4.9	(1.7)	14	3.86	(1.7)	7	3.10	(3.4)	7.7

[a] Edwards et al (1978).
[b] Biggin and Enderby (1981).
[c] McGreevy and Mitchell (1982).
[d] Biggin et al (1984).

explanation along the lines of thermal disorder may be appropriate. This, however, needs to be reconciled with the fact that the principal peak in the $+-$ partial is less susceptible to changes in temperature.

A second distinguishing feature is the lack of the prominent pre-peak found by Biggin and Enderby in $S_{ZnZn}(Q)$ at $Q \simeq 1 \text{ Å}^{-1}$. There is, as we have pointed out, strong evidence to support the existence of a broad hump or shoulder in this region for $S_{NiNi}(Q)$ but this feature is an order of magnitude smaller. Thus one concludes that although the local structure around the Ni^{2+} ion resembles that around the Zn^{2+} ion, there is in contrast, an absence of any intermediate range correlation of the Ni^{2+} ions. Furthermore, there is only a weak minimum between the principal and second peaks in $g_{NiNi}(r)$. This suggests an enhanced mobility of the cations in the $NiCl_2$ case, with increased migration between the tetrahedral sites. This view is supported by the fact that the electrical conductivity of $NiCl_2$ at the melting point is considerably larger than that of $ZnCl_2$ at the melting point. This could of course be a thermally induced process and it would be interesting to observe whether or not the large pre-peak in $ZnCl_2$ persists at higher temperatures.

The trend in the cation–anion separation from Ba (largest ion) to Zn (smallest ion) appears to correlate very well with a simple ion size effect and, indeed, is close to the sum of the simple ionic radii. The trend is broken at Ni, however, and both Ni and Mg exhibit an increase in the separation with decreasing ion size. This could well be indicative of the polarisation effects brought about by the high polarising powers of small ions such as nickel and magnesium. Computer simulation studies of a $1:1$ molten salt (Dixon and Sangster, 1975) have shown that the inclusion of polarisation terms in a model potential enhances the differences between $g_{++}(r)$ and $g_{--}(r)$ and reduces the principal peak height in $g_{+-}(r)$. Further experiments on materials containing small, polarising cations in the presence of large polarisable anions are now needed to quantify the extent to which polarisation effects modify the structure.

The anion structure is remarkably stable over the entire range of cation species, the separation remaining close to the sum of the rigid ion radii (3.62 Å) and the coordination number persisting at around eight. The high coordination number of 12 observed in $MgCl_2$ does seem to be an exception and may be related to the fact that it is obtained by integrating up to a rather high minimum and associated with a shouldered peak in the radial distribution function.

In conclusion, this study confirms that liquid $NiCl_2$ ionises into a Ni^{2+} ion accompanied by two Cl^- ions. The small Ni ion is accommodated in a tetrahedrally coordinated site in a Cl^- structure that does not differ extensively from that found in the solid. Liquid $NiCl_2$ closely resembles liquid $ZnCl_2$ although the prominent pre-peak in the Zn–Zn structure factor is absent and the structural ordering is decreased, possibly due to thermal effects at the elevated temperature. Effects other than ion size, and possibly including polarisation, are needed to explain the details of the structure.

References

Biggin S and Enderby J E 1981 *J. Phys. C: Solid State Phys.* **14** 3129 and 3577
Biggin S, Gay M and Enderby J E 1984 *J. Phys. C: Solid State Phys.* **17** 977
Dixon M and Sangster M J L 1975 *J. Phys. C: Solid State Phys.* **8** L8
Edwards F G, Enderby J E, Howe R A and Page D I 1975 *J. Phys. C: Solid State Phys.* **8** 3483
Edwards F G, Howe R A, Enderby J E and Page D I 1978 *J. Phys. C: Solid State Phys.* **11** 1053
McGreevy R L and Mitchell E W J 1982 *J. Phys. C: Solid State Phys.* **15** 5537
Waseda Y 1980 *Structure of Non-Crystalline Materials: Liquids and Amorphous Solids* (London: McGraw-Hill).
Wyckoff R W G 1963 *Crystal Structures* 2nd edn. vol 1 (New York: Interscience)